

## Static model of the quark potential. II

Roscoe Giles

*Center for Theoretical Physics, Laboratory for Nuclear Sciences, Massachusetts Institute of Technology, Cambridge, Massachusetts 02139*

Larry McLerran

*Stanford Linear Accelerator Center, Stanford University, Stanford, California 94305*

(Received 9 October 1979)

We use a semiclassical method to calculate the potential energy of a heavy quark-antiquark pair. We also present numerical results for the average distribution of gluons which surround the quark-antiquark pair.

### I. INTRODUCTION

A method for calculating the effects of interactions between heavy quarks within the framework of quantum chromodynamics (QCD) would be of great utility.<sup>1-11</sup> For heavy-quark systems, the problem of determining an effective QCD interaction potential is perhaps most clearly isolated from the intricacies of the field-theoretical bound-state problem. As quark masses increase, moreover, the corresponding QCD interaction strengths decrease, and the calculation of the potential in perturbation theory becomes more reliable. For systems such as the  $J/\psi$  (Refs. 12-17) or  $\Upsilon$  (Refs. 18-20) families of resonances, however, the strong-interaction strength  $\alpha_s$  is  $\sim 1-2$ .<sup>21-25</sup> Only heavy-quark bound states of much greater mass might be expected to be adequately described by a Coulomb potential. For systems where  $\alpha_s$  is of moderate strength, such as the  $J/\psi$  and  $\Upsilon$ , we must develop calculational techniques that go beyond those which are appropriate to weak coupling.

A feature which distinguishes QCD from QED is that even static sources will induce an enveloping cloud of radiation.<sup>26</sup> This cloud arises from non-vanishing couplings of stationary quark sources and transverse gluon degrees of freedom. Such couplings may ultimately be responsible for confinement through nonperturbative mechanisms and certainly yield numerically significant contributions to the quark-antiquark potential for intermediate coupling strengths.

In Ref. 8, henceforth referred to as "I", we introduced an approximation which may prove useful for describing the gluon cloud that surrounds a static  $q\bar{q}$  pair. The approximation is an analog of the Tomonaga approximation of nuclear physics.<sup>27-31</sup> In I, we demonstrated that this method together with renormalization-group improvement accurately approximates the known results of perturbation theory up to and including effects of at least order  $\alpha_s^4 \ln \alpha_s$  (Ref. 5).

In the present paper we present some results of

numerical calculations of the gluonic structure of  $q\bar{q}$  states in this static limit. Our purpose here is not so much to accurately determine a  $q\bar{q}$  effective potential—indeed the extraction of an effective potential from our static-quark calculation requires detailed consideration of velocity-dependent effects<sup>32-34</sup>—but rather to investigate the structure of the non-Abelian gluon cloud generated in such states. We also hope that the techniques discussed here may provide a first tentative step along the road toward the understanding of the structure of heavy-quark bound states.

The outline of this paper is as follows: In Sec. II, we briefly review the results of I. The numerical solutions of the equations derived in Sec. II are discussed in Sec. III. In Sec. III we also describe the configuration-space structure of the gluon cloud, its charge density, and its chromoelectric and chromomagnetic fields. The detailed numerical analysis of Appendices A-E are utilized in this section. Section IV offers a summary and discussion of our results.

### II. THE TOMONAGA APPROXIMATION

In this section, we consider the interaction of stationary, pointlike, spinless  $SU(N)$  color sources. These sources are described by charge operators  $Q_a$  and  $\bar{Q}_a$  satisfying the algebra

$$Q_a Q_b = \frac{1}{2N} \delta_{ab} + \frac{1}{2} d_{abc} Q_c + \frac{i}{2} f_{abc} Q_c, \quad (2.1a)$$

$$\bar{Q}_a \bar{Q}_b = \frac{1}{2N} \delta_{ab} - \frac{1}{2} d_{abc} \bar{Q}_c + \frac{i}{2} f_{abc} \bar{Q}_c. \quad (2.1b)$$

The indices  $a, b$  range from 1 to  $N^2 - 1$ . The charge density corresponding to these operators is

$$\rho_{\text{quark}}^a(\vec{r}) = Q^a \delta^{(3)}(\vec{r} - \frac{1}{2} \vec{R}) + \bar{Q}^a \delta^{(3)}(\vec{r} + \frac{1}{2} \vec{R}), \quad (2.2)$$

with coordinates chosen so that the quark resides at  $\vec{R}/2$ , and the antiquark at  $-\vec{R}/2$ . In the analysis which follows, we shall measure distances in units of  $|\vec{R}|$ , corresponding to setting  $|\vec{R}| = 1$ .

The interactions of these static quarks are conveniently described by the QCD Coulomb-gauge Hamiltonian. We do not address the problems of the Gribov-Mandelstam ambiguities that may arise in the implementation of this gauge.<sup>35,36</sup> Such ambiguities appear to be most significant in regions characterized by "large fields" where our approximation is also subject to large corrections arising from many other sources.<sup>37-39</sup> Our calculations show no hint of any such ambiguities.

In the Coulomb gauge the independent degrees of freedom correspond to transverse gluons. The interactions include cubic and quartic transverse-gluon couplings, and instantaneous Coulomb interactions of the quarks and gluons. The full set of instantaneous Coulombic interactions are nonpolynomial in the gluon fields and, even in the static limit, are the source of nonvanishing interactions of quarks and transverse gluons.

These interactions arise from the following term in the Hamiltonian,

$$V_{\text{Coul}} = \frac{1}{2} \sum_a \int d^3r \bar{E}_L^a(\vec{r})^2, \quad (2.3)$$

where  $\bar{E}_L^a(\vec{r})$  ( $a=1, \dots, N^2-1$ ) is the longitudinal chromoelectric field. The longitudinal chromoelectric field is a dependent field which may be determined in terms of the quark and transverse-gluon degrees of freedom by solving Gauss's law:

$$D_j E_j = \nabla_j E_j^L + g A_j \times E_j^L + g A_j \times E_j^L = \rho_{\text{quark}}, \quad (2.4a)$$

or

$$D_j E_j^L = \rho_{\text{quark}} + g E_j^L \times A_j \equiv J^0. \quad (2.4b)$$

We use the notation

$$(A \times B)^a = f^{abc} A_b B_c. \quad (2.5)$$

In these equations,  $\bar{E}_\perp$  is the transverse chromoelectric field and  $J^0$  is the charge density arising from quarks and transverse gluons. Using Eq. (2.4b) in Eq. (2.3), we obtain

$$V_{\text{Coul}} = \frac{1}{2} \int d^3r d^3r' J_a^0(\vec{r}) \Phi_{ab}(\vec{r}, \vec{r}') J_b^0(\vec{r}'), \quad (2.6)$$

where the Coulomb energy operator  $\Phi_{ab}(\vec{r}, \vec{r}')$  is

$$\Phi = (\nabla \cdot D)^{-1} (-\nabla^2) (\nabla \cdot D)^{-1}, \quad (2.7)$$

or

$$\begin{aligned} \Phi_{ab}(\vec{r}, \vec{r}') &= \frac{1}{-\nabla^2}(\vec{r}, \vec{r}') \delta_{ab} \\ &+ g f^{acb} \frac{1}{-\nabla^2} A_{cj} \bar{\nabla}_j \frac{1}{-\nabla^2}(\vec{r}, \vec{r}') + O(g^2). \end{aligned} \quad (2.8)$$

In perturbation theory, the leading-order coupling

of transverse gluons to the  $q\bar{q}$  pair is given by the second term in Eq. (2.8).

In the stationary-spinless-quark limit, quark recoil and spin effects vanish. The spatial and spin structure of the quark-antiquark sources are time independent and do not induce correlations in the spatial wave functions of successively emitted or absorbed gluons. For this situation, as was argued in I, a reasonable approximation for the description of the gluons may be obtained by supposing that all gluons share a single spatial wave function. Note, however, that because the quark and antiquark reside in a low-dimensional representation of the  $SU(N)$  color group, color recoil effects are expected to be very important. Therefore, an essential ingredient of any approximation to the description of such quarks must be the operator structure of the color charges of quarks and gluons.

The Tomonaga approximation discussed in I is tailored to fit this body of constraints. The Hamiltonian which describes quarks and gluons is diagonalized in a subspace of states consisting of arbitrary numbers of gluons of arbitrary colors, all sharing a common spatial wave function  $\psi_j(\vec{k})$ . The operator structure of the quark and antiquark charges is exactly maintained. As shown in I, matrix elements of the Hamiltonian in this subspace of states correspond to matrix elements of an effective Hamiltonian which describes  $N^2-1$  "coordinate" degrees of freedom (corresponding to the  $N^2-1$  colors of gluons) interacting with the  $N^2-1$  color "spins" of the quark and antiquark.

In deriving the effective Hamiltonian presented in I, we made a further severe truncation of the full Hamiltonian as it would appear in the Tomonaga approximation. We retained only the leading interaction term represented by the second term in Eq. (2.8). The neglected terms include modifications of transverse-gluon propagation arising from the background field of the quark charges and from mutual interactions of transverse gluons. We do, however, allow for a shift of local operator expectation values from their vacuum values, and in this sense we are performing a mean-field approximation.

The resulting effective Hamiltonian is

$$\mathcal{H} = \mathcal{E}_0 [a^\dagger \cdot a + \beta Q \cdot \bar{Q} + \bar{\gamma} (Q \times \bar{Q}) \cdot (a + a^\dagger)], \quad (2.9)$$

where  $a_a^\dagger$  and  $a_a$  ( $a=1, \dots, N^2-1$ ) are one-gluon creation and annihilation operators. The commutation relations of  $a$ ,  $a^\dagger$ ,  $Q$ , and  $\bar{Q}$  are, in addition to those given in Eqs. (2.1a) and (2.1b),

$$[a_a, a_b^\dagger] = \delta_{ab}, \quad (2.10a)$$

$$\begin{aligned} [a_a, a_b] &= [a_a, Q_b] = [a_a^\dagger, Q_b] \\ &= [a_a, \bar{Q}_b] = [a_a^\dagger, \bar{Q}_b] = 0. \end{aligned} \quad (2.10b)$$

The three numbers  $\mathcal{E}_0$ ,  $\bar{\beta}$ , and  $\bar{\gamma}$  are functionals of the classical gluon wave function  $\bar{\psi}$ . The Hamiltonian is diagonalized for arbitrary  $\mathcal{E}_0$ ,  $\bar{\beta}$ , and  $\bar{\gamma}$ , allowing us to obtain its ground state  $|\Omega\rangle$ . The wave function  $\bar{\psi}$  is determined by minimizing the ground-state energy  $\mathcal{E}_0[\bar{\psi}]$  with respect to  $\bar{\psi}$ , subject to the normalization condition

$$\int \frac{d^3k}{(2\pi)^3 2k} \bar{\psi}^*(\vec{k}) \cdot \bar{\psi}(\vec{k}) = 1. \tag{2.11}$$

The variational calculation performed in I gives

$$\bar{\psi}(\vec{k}) = g^3 P \frac{\vec{J}(\vec{k})}{k + \Lambda}, \tag{2.12}$$

where  $\Lambda$  is a Lagrange multiplier which enforces Eq. (2.11). The current  $\vec{J}(\vec{k})$  is the Fourier transform of the spatial factors which couple to  $\vec{A}^a(\vec{r})$  in Eq. (2.8) (Fig. 1),

$$\begin{aligned} \vec{J}(\vec{k}) = \int d^3r e^{-i\vec{k}\cdot\vec{r}} & \left[ \frac{1}{4\pi|\vec{r}-\vec{r}_1|} - \frac{1}{4\pi|\vec{r}_1-\vec{r}_2|} \right] \\ & \times \vec{\nabla} \left( \frac{1}{4\pi|\vec{r}-\vec{r}_2|} - \frac{1}{4\pi|\vec{r}_1-\vec{r}_2|} \right). \end{aligned} \tag{2.13}$$

The quantity  $P$  is the ratio of ground-state expectation values

$$P \equiv \frac{\langle \Omega | (Q \times \vec{Q}) \cdot (a + a^\dagger) | \Omega \rangle}{2 \langle \Omega | a^\dagger \cdot a | \Omega \rangle}. \tag{2.14}$$

The Lagrange multiplier  $\Lambda$  must be determined so that  $\bar{\psi}$  is normalized to one. As the solution for  $\Lambda$  as a function of  $g^2$  involves the intermediate step of diagonalizing  $\mathcal{H}$  (the couplings of which depend on  $\Lambda$ ), the problem of determining  $\Lambda$  is complex and must be solved numerically.

In the following sections, we discuss the solution of this model theory. We determine  $\Lambda$  as a function of  $\alpha_s$ , find the dependence of  $\bar{\psi}$  on  $\alpha_s$ , and calculate the gluon wave function  $\bar{\psi}$ .

### III. RESULTS

The coefficients  $\mathcal{E}_0$ ,  $\bar{\beta}$ , and  $\bar{\gamma}$  may be computed in terms of functions  $C_n(\Lambda)$  as

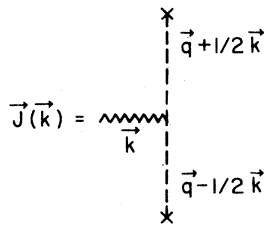


FIG. 1. The current  $\vec{J}(\vec{k})$ .

$$\mathcal{E}_0 = \frac{C_1 - \Lambda C_2}{C_2}, \tag{3.1}$$

$$\bar{\beta} = \frac{g^2}{4\pi} \frac{C_2}{C_1 - \Lambda C_2}, \tag{3.2}$$

and

$$\bar{\gamma} = -g^3 \frac{C_1 C_2^{1/2}}{C_1 - \Lambda C_2}. \tag{3.3}$$

The functions  $C_n(\Lambda)$  are obtained from a classical current  $\vec{J}$  as

$$C_n(\Lambda) = \int \frac{d^3k}{(2\pi)^3 2k} \vec{J}^2(\vec{k}) \left( \frac{1}{k + \Lambda} \right)^n. \tag{3.4}$$

The parameter  $\Lambda$  must be adjusted so that the gluon wave function is normalized to one,

$$g^6 C_2(\Lambda) P^2 = 1. \tag{3.5}$$

To solve this equation for  $\Lambda$ ,  $\mathcal{H}$  must be diagonalized for arbitrary  $\Lambda$ . The root of Eq. (3.5) is then determined by successive iterations. We have diagonalized  $\mathcal{H}$  numerically in the basis discussed in I and determined  $\Lambda$ . To perform the numerical analysis, we first obtained expressions for  $C_n(\Lambda)$  that could be easily evaluated. In Appendices A-C, the coefficients in the series expansion

$$C_1(\Lambda) = \frac{1}{(4\pi)^3} \left( \sum_{p=0}^{\infty} \frac{\alpha_p \Lambda^p}{p!} + \ln \Lambda \sum_{p=1}^{\infty} \frac{\beta_p \Lambda^p}{p!} \right) \tag{3.6}$$

are determined. The coefficients  $C_n(\Lambda)$  are derived from

$$C_n(\Lambda) = \frac{(-)^{n-1}}{n!} \left( \frac{d}{d\Lambda} \right)^{n-1} C_1(\Lambda). \tag{3.7}$$

We have checked this tedious analytic evaluation of  $C_1(\Lambda)$  by comparing Eq. (3.6) with the asymptotic series for large  $\Lambda$  and by directly evaluating Eq. (3.4) with the Monte Carlo numerical integration routine Vegas.<sup>40</sup> The asymptotic series for  $C_1(\Lambda)$  is derived in Appendix D. Plots of  $C_1$  and  $C_2$  are given in Figs. 2 and 3. Both  $C_1$  and  $C_2$  are rapidly decreasing functions of  $\Lambda$  for  $0 < \Lambda < 1$  and are not well approximated by their lowest-order terms in the expansion of Eq. (3.6),

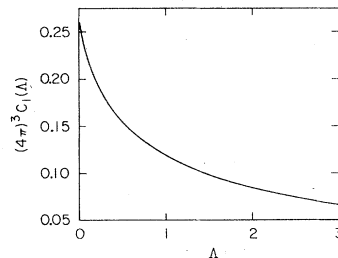
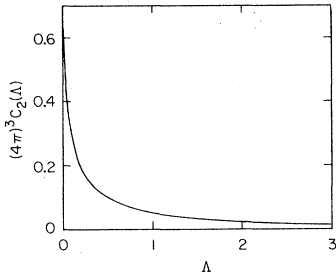


FIG. 2. The function  $C_1(\Lambda)$ .

FIG. 3. The function  $C_2(\Lambda)$ .

$$C_1(\Lambda) = \frac{1}{(4\pi)^3} \left[ 3 \left( 1 - \frac{\pi^2}{12} \right) + \frac{2}{3\pi} \Lambda \ln \Lambda \right], \quad (3.8)$$

$$C_2(\Lambda) = -\frac{1}{(4\pi)^3} \frac{2}{3\pi} \ln \Lambda, \quad (3.9)$$

for  $\Lambda \gtrsim \frac{1}{2}$ .

We have used the functions  $C_1$  and  $C_2$  in the diagonalization of  $\mathcal{H}$  which was carried out numerically for SU(3). We varied the parameter  $\Lambda$  until the normalization condition [Eq. (3.9)] was satisfied. This procedure gave us a relationship between  $\Lambda$  and  $\alpha_s$ ,

$$\Lambda = \frac{3}{2} \alpha_s G(\alpha_s). \quad (3.10)$$

The lowest-order perturbation-theory value for  $\Lambda$  was found in I to be  $\Lambda = \frac{3}{2} \alpha_s$ , so that  $G(\alpha_s)$  satisfied

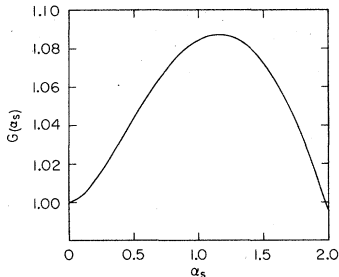
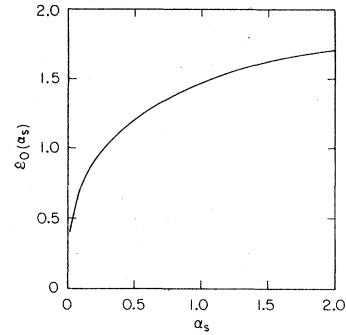
$$G(0) = 1. \quad (3.11)$$

To an accuracy of 10%,  $G(\alpha_s) = 1$  for  $0 \leq \alpha_s \leq 2$ . A plot of  $G(\alpha_s)$  is shown in Fig. 4.

The quantities  $\mathcal{E}_0$ ,  $\bar{\beta}$ , and  $\bar{\gamma}$  as functions of  $\alpha_s$  are shown in Figs. 5–7. Several features of these functions are noteworthy. For small  $\alpha_s$ , both  $\mathcal{E}_0$  and  $\bar{\beta}$  rise rapidly from zero while the parameter  $\bar{\gamma}$  rises slowly from zero. For intermediate values of  $\alpha_s \sim 1-2$ ,  $\mathcal{E}_0$  levels off and  $\bar{\beta}$  and  $\bar{\gamma}$  vary linearly. In fact, for large  $\alpha_s$ ,

$$\bar{\beta}(\alpha_s) \sim -\bar{\gamma}(\alpha_s). \quad (3.12)$$

The perturbation-theory values of  $\mathcal{E}_0$ ,  $\bar{\beta}$ , and  $\bar{\gamma}$

FIG. 4. The function  $G(\alpha_s)$ .FIG. 5. The function  $\mathcal{E}_0(\alpha_s)$ .

are given by Eqs. (3.1)–(3.3) and Eqs. (3.8) and (3.9). With  $\Lambda = \frac{3}{2} \alpha_s$

$$\mathcal{E}_0 \cong -\frac{9}{4}\pi \left( 1 - \frac{\pi^2}{12} \right) \frac{1}{\ln \alpha_s}, \quad (3.13)$$

$$\bar{\beta} \cong \frac{1}{\frac{9}{4}\pi \left( 1 - \frac{\pi^2}{12} \right)} \alpha_s \ln \alpha_s, \quad (3.14)$$

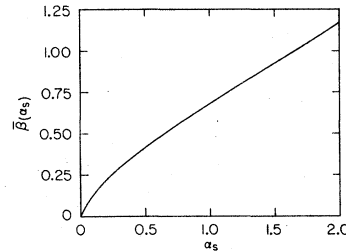
and

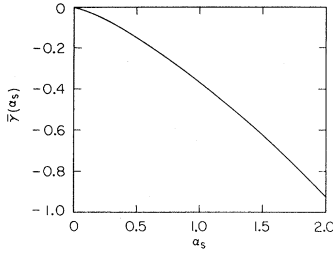
$$\bar{\gamma} \cong -\alpha_s^{3/2} \left( -\frac{2}{3\pi} \ln \alpha_s \right)^{1/2}. \quad (3.15)$$

For  $\alpha_s \gtrsim \frac{1}{2}$ ,  $\mathcal{E}_0$ ,  $\bar{\beta}$ , and  $\bar{\gamma}$  show significant deviations from their perturbation-theory values.

The magnitude of  $\bar{\gamma}$  determines the strength of mixing between states with different numbers of occupied coherent gluon modes. The slow increase in the magnitude of  $\bar{\gamma}(\alpha_s)$  for  $\alpha_s \approx 1-2$  leads to a small gluon content of the ground-state wave function. In fact, for  $\alpha_s \approx 2$ , the average value of the number operator  $\langle \Omega | a^\dagger \cdot a | \Omega \rangle$  is less than 0.25 as shown in Fig. 8.

The amplitudes for the ground-state wave function to be in the states  $|0\rangle$ ,  $|1\rangle$ , and  $|2\rangle$  are shown in Fig. 9. The amplitude for  $|2\rangle$  reaches only  $\sim 0.10-0.15$  at  $\alpha_s \sim 2$ . The contribution to the ground-state energy from these various modes is  $\sim (\text{amplitude})^2$ , so that for  $\alpha_s \approx 2$ , the contribution from modes with  $n \geq 2$  is  $\delta E \leq 1-2\%$ . For this range of  $\alpha_s$  the system is adequately described as a mixture of the two total color-singlet states:

FIG. 6. The function  $\bar{\beta}(\alpha_s)$ .

FIG. 7. The function  $\bar{\gamma}(\alpha_s)$ .

|singlet quark pair, no gluons> and |octet quark pair, one gluon>.

The function  $F(\alpha_s)$  which measures the deviation of  $E$  from its Coulombic dependence on  $\alpha_s$ ,

$$E(R) = -\frac{T_2}{R} \alpha_s F(\alpha_s), \quad (3.16)$$

is shown in Fig. 10. The function  $F(\alpha_s)$  rises from its value of 1 at  $\alpha_s = 0$  and acquires a linear dependence for  $\alpha_s \sim 1-2$ . For  $\alpha_s \lesssim \frac{1}{2}$ , the function  $F(\alpha_s)$  is not well approximated by its perturbation-theory value of

$$F(\alpha_s) = 1 + \frac{27}{8} \left(1 - \frac{\pi^2}{12}\right) \alpha_s^2 + \frac{9}{4\pi} \alpha_s^3 \ln \alpha_s + O(\alpha_s^3). \quad (3.17)$$

Associated with the gluon wave function  $\vec{\psi}(\vec{k})$  are various classical fields in coordinate space. These are related to effective field operators in the Tomonaga approximation. In matrix elements involving such states we have

$$\vec{A}_a(\vec{x}) = \vec{Q}(\vec{x})(a_a + a_a^\dagger), \quad (3.18a)$$

$$\vec{E}_{1a}(x) = \vec{E}_1(\vec{x})i(a_a^\dagger - a_a), \quad (3.18b)$$

$$\vec{B}_a(x) = \vec{Q}(x)(a_a + a_a^\dagger), \quad (3.18c)$$

$$\rho_a^{\text{gluon}}(x) = \rho(\vec{x})ia \times a^\dagger, \quad (3.18d)$$

where the  $c$ -number fields  $\vec{Q}$ ,  $\vec{E}_1$ ,  $\vec{B}$ , and  $\rho$  are

$$\vec{Q}(\vec{x}) = \int \frac{d^3k}{(2\pi)^3 2|\vec{k}|} e^{i\vec{k}\cdot\vec{x}} \vec{\psi}(\vec{k}), \quad (3.19a)$$

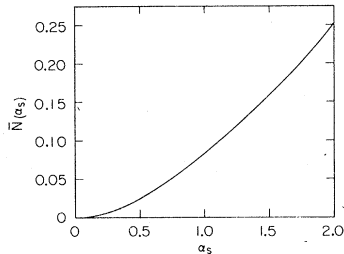
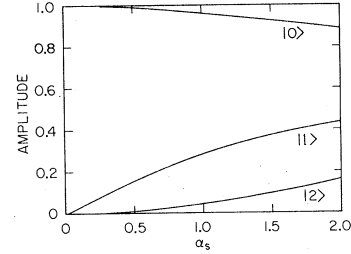
FIG. 8. The expectation value of the gluon occupation number  $\bar{N}(\alpha_s)$ .

FIG. 9. The amplitude of the ground-state wave function to be in the states |0&gt; (top line), |1&gt; (middle line), and |2&gt; (bottom line).

$$\vec{E}_1(\vec{x}) = \int \frac{d^3k}{(2\pi)^3 2|\vec{k}|} |\vec{k}| e^{i\vec{k}\cdot\vec{x}} \vec{\psi}(\vec{k}), \quad (3.19b)$$

$$\vec{Q}(\vec{x}) = \vec{\nabla} \times \vec{Q}(\vec{x}), \quad (3.19c)$$

$$\rho(\vec{x}) = \vec{E}_1(\vec{x}) \cdot \vec{Q}(\vec{x}). \quad (3.19d)$$

Figures 11-18 show plots of  $Q^2(x)$ ,  $E_1^2(x)$ ,  $|Q(x)|$ , and  $\rho(x)$  as functions of cylindrical variables  $r_1$  and  $z$  for  $\Lambda=0$  and  $\Lambda=3$ . These fields are azimuthally symmetric. The overall scale of the magnitude of the various fields is arbitrary, the important comparison being the relative shape of the distributions. The quarks are located along the  $z$  axis at positions which are obvious in the figures.

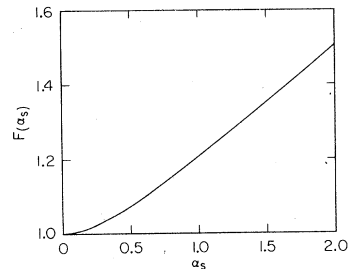
For any  $\Lambda \neq 0$  the asymptotic behavior of the various fields can be deduced. For large  $r$ , the potential  $\vec{Q}(\vec{x})$  falls like  $1/r^2$  while  $\vec{E}_1$  and  $\vec{B}$  fall like  $1/r^3$ . Thus, the resulting gluon charge density falls like  $1/r^4$ .

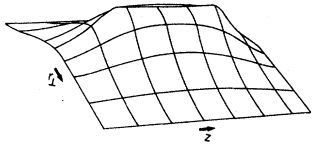
The normalization condition on the wave function is precisely the condition

$$\int d^3x \rho(\vec{x}) = 1. \quad (3.20)$$

For  $\Lambda=0$ ,  $\vec{Q}$  behaves asymptotically as  $1/r$ , while  $E_1$  and  $B$  behave as  $1/r^2$ . At the point  $\Lambda=0$ ,  $\rho$  becomes non-normalizable, accounting for the logarithmic divergence in  $C_2(\Lambda)$  as  $\Lambda \rightarrow 0$ .

Near the quark ( $\vec{x} = \vec{r}_i$ ) the dominant contributions to  $Q$ ,  $E_1$ , and  $B$  come from the large  $|\vec{k}|$  region of integration:  $|\vec{k}| \gg \Lambda$ . The analysis of Appendix E then indicates that  $\vec{Q} \sim \text{constant}$ ,  $|\vec{E}_1|$

FIG. 10. The function  $F(\alpha_s)$ .

FIG. 11. The field  $Q^2$  for  $\Lambda=0$ .

and  $\rho \sim 1/|\vec{x} - \vec{r}_i|$ , and  $|\vec{\mathcal{G}}| \sim \sin\theta/|\vec{x} - \vec{r}_i|$ , where  $\theta$  is the usual polar angle.

The magnetic field is singular near the quarks and its value depends on the path of approach to the position of the quark. Along the line separating the quarks, the field is zero. As  $\Lambda$  increases, the fields concentrate nearer the quarks.

The charge distribution resembles the distribution of transverse electric field. The charge is concentrated near and between the quarks for small  $\Lambda$ , and increasingly near the quarks for increasing  $\Lambda$ .

For small  $\Lambda$  the transverse electric field is spread out in the region between the quarks. Increasing  $\Lambda$  increases the concentration of the electric fields near the quarks.

As the  $q\bar{q}$  separation changes, the magnitudes of fields all scale with powers of  $1/R$  corresponding to their canonical dimension. That is,

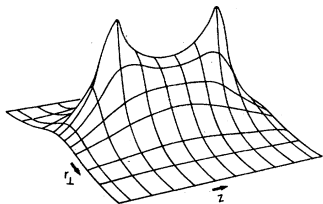
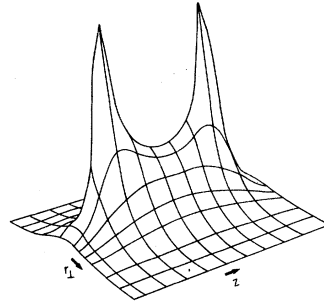
$$\vec{\mathcal{G}}(\alpha_s, R, \vec{x}) = \frac{1}{R} \vec{\mathcal{G}}\left(\alpha_s, \frac{\vec{x}}{R}\right), \quad (3.21a)$$

$$\vec{\mathcal{E}}_1(\alpha_s, R, \vec{x}) = \frac{1}{R^2} \vec{\mathcal{E}}_1\left(\alpha_s, \frac{\vec{x}}{R}\right), \quad (3.21b)$$

$$\vec{\mathcal{G}}(\alpha_s, \vec{R}, \vec{x}) = \frac{1}{R^2} \vec{\mathcal{G}}\left(\alpha_s, \frac{\vec{x}}{R}\right), \quad (3.21c)$$

$$\rho(\alpha_s, \vec{R}, \vec{x}) = \frac{1}{R^3} \rho\left(\alpha_s, \frac{\vec{x}}{R}\right). \quad (3.21d)$$

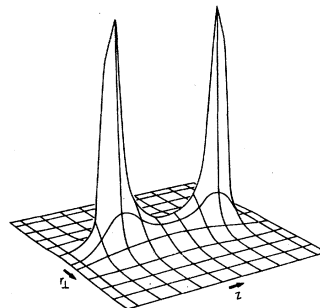
Thus, as quarks are separated, the overall shapes of the field distributions are unchanged but magnitudes decrease. Note, however, that an observer sitting at a fixed point in space as the pair is separated does see both the overall scale decrease and effects due to the change in his scaled coordinate  $\vec{x}/R$ .

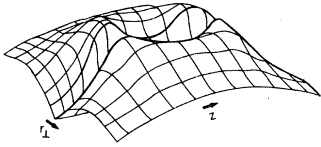
FIG. 12. The field  $Q^2$  for  $\Lambda=3$ .FIG. 13. The field  $\mathcal{E}_1^2$  for  $\Lambda=0$ .

#### IV. CONCLUSIONS

In this section, we summarize our results and consider their implications for the physics of heavy-quark systems as described by QCD. Our approximation scheme is designed to give a reasonable representation of the gluonic structure generated in the presence of stationary quantum charge sources. The validity of the Tomonaga approximation rests on the notion that in the absence of quark spatial and spin recoil effects, gluons of a single space-spin wave function will be dominant. The truncation of the Coulomb-gauge Hamiltonian to the leading (in perturbation theory) gluon-source interaction of Eq. (2.8) is motivated primarily by the desire for simplicity and certainly is appropriate for sufficiently small coupling. Ultimately, the reliability of our approximation scheme for increasing  $\alpha_s$  can best be checked only by computing higher-order effects.

With our approximations, the following picture of the quark-antiquark state emerges for couplings  $\alpha_s \approx 1-2$ : The total color-singlet ground state is mostly pure  $(q\bar{q})$  singlet with a small admixture of the one-gluon state  $(q\bar{q})_8(G)_8$ . The amplitudes for components containing more than one gluon are tiny despite the fact that the Tomonaga approximation allows for their presence. We interpret this result as a dynamical consequence of the theory. Even at relatively large coupling ( $\alpha_s \sim 2$ )

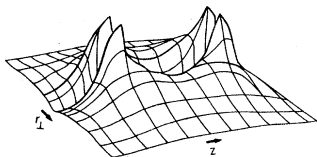
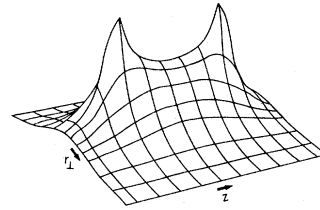
FIG. 14. The field  $\mathcal{E}_1^2$  for  $\Lambda=3$ .

FIG. 15. The field  $|G|$  for  $\Lambda=0$ .

there is no dramatic increase in the gluonic component of the lowest-lying singlet state. This result, though perhaps disappointing from the point of view of one looking for dramatic behavior suggestive of an approach to confinement, is in accord with the naive quark-model picture of such states as predominantly pure  $q\bar{q}$ .

The behavior of the energy as a function of  $\alpha_s$  is also undramatic. In the region of  $\alpha_s \sim 1-2$ , it deviates less from the Coulomb form than might be suggested by the extension of the order  $\alpha_s^4 \ln \alpha_s$  perturbative results beyond their obvious domain of validity. Only the shape of the gluon wave function appears sensitive to the strength of the coupling. This dependence is the source of nonanalyticity in coupling at  $\alpha_s = 0$ .

The point in coupling at which our approximation scheme breaks down is not clear. The small average gluon number in the region  $\alpha_s \sim 1-2$  suggests that corrections in this region will be small. The Tomonaga approximation itself (which becomes the Tamm-Dancoff approximation when restricted to  $n_{\text{gluon}} = 1$ ) becomes unreliable when mechanisms which tend to disperse gluons in space-spin are important. Such effects are certainly present in QCD (for example, in the interactions of gluons with one another) but may be expected to be small. One term which deserves particular attention is that representing the Coulomb interaction between a gluon and one of the sources (Fig. 19). It is this term in the classical Hamiltonian which is responsible for the Mandula instability of the Coulomb field for a classical color source of sufficient strength,  $\alpha_s \geq \frac{3}{2}$  (Refs. 37 and 38). We might expect that this instability should be reflected in the quantum theory for sufficiently large coupling if the corresponding term in the Hamiltonian is included in our approximation. This expectation leads to an upper bound on the value of  $\alpha_s$  at which we can have any real confidence in our results.

FIG. 16. The field  $|G|$  for  $\Lambda=3$ .FIG. 17. The field  $\rho$  for  $\Lambda=0$ .

Note, however, that the instability is a *single-charge* effect and may not dramatically affect the interaction energy between charges.

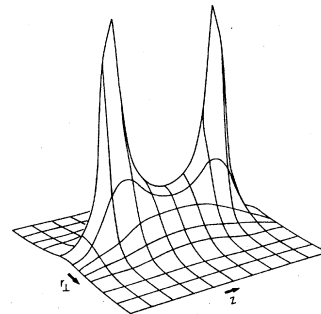
The techniques introduced in I and analyzed here might be expected to be of use phenomenologically in the characterization of properties of heavy-quark bound states. It is important in this connection to reiterate the observation that velocity-dependent effects in the finite-mass case are not trivial and the extraction of an effective  $q\bar{q}$  potential is complex.<sup>32-34</sup> A more fruitful application of our techniques might be the investigation of spin-dependent forces induced via the gluon cloud.

#### ACKNOWLEDGMENTS

The authors gratefully acknowledge useful conversations with S. Adler, M. Baker, L. S. Brown, M. Dine, S. Ellis, R. Freedman, E. Henley, J. Mandula, J. Richardson, P. Sikivie, M. Weinstein, W. Weisberger, and L. Willets. This work was supported by the Department of Energy under Contract Nos. DE-AC03-76SF00515 and EY-76-COZ-3069.

#### APPENDIX A

In this appendix, we find an integral representation for the current  $\vec{J}(\mathbf{k})$ . We begin by recalling that the current can be computed from the Feynman graph of Fig. 1 with the result

FIG. 18. The field  $\rho$  for  $\Lambda=3$ .

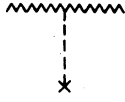


FIG. 19. The Coulomb interaction of a gluon and a single charged source.

$$\vec{J}(\vec{k}) = 2i \int \frac{d^3q}{(2\pi)^3} e^{i\vec{q}\cdot\vec{R}} \left( \vec{q} - \vec{k} \frac{1}{k^2} \vec{k} \cdot \vec{q} \right) \times \frac{1}{(\vec{q} + \frac{1}{2}\vec{k})^2} \frac{1}{(\vec{q} - \frac{1}{2}\vec{k})^2}. \quad (\text{A1})$$

In this equation, the separation of the quarks is  $R$ . The Coulomb propagators in Eq. (A1) may be combined using a Feynman parameter to yield

$$\vec{J}(\vec{k}) = 2i \left( \hat{R} - \vec{k} \frac{1}{k^2} \vec{k} \cdot \hat{R} \right) \times \int_0^1 d\alpha e^{i(\alpha-1/2)\vec{k}\cdot\vec{R}} \times \int \frac{d^3q}{(2\pi)^3} e^{i\vec{q}\cdot\vec{R}} \vec{q} \cdot \hat{R} [\vec{q}^2 + \alpha(1-\alpha)\vec{k}^2]^{-2}. \quad (\text{A2})$$

The integrations over  $d^3q$  give

$$C_p(\Lambda) \equiv \int \frac{d^3k}{(2\pi)^3 2k} \frac{1}{(k+\Lambda)^p} \vec{J}^2(\vec{k}). \quad (\text{B1})$$

We shall proceed by deriving a Mellin integral representation for  $C_p$  as a function of  $\Lambda$ . [In Appendix C we shall use this Mellin representation to evaluate the coefficients of a Taylor-series expansion for  $C_p(\Lambda)$  in powers of  $\Lambda$  and powers of  $\Lambda$  times  $\ln\Lambda$ . We shall also use this representation to obtain an asymptotic expansion in inverse powers of  $\Lambda$  and inverse powers of  $\Lambda$  times  $\ln\Lambda$ .]

We begin by observing that

$$C_p(\Lambda) = (-)^{p-1} \left( \frac{1}{p!} \right) \left( \frac{d}{d\Lambda} \right)^{p-1} C_1(\Lambda), \quad (\text{B2})$$

so that without loss of generality we may consider only  $C_1(\Lambda)$ . Using Eq. (A5) with  $R=1$ , we have

$$C_1(\Lambda) = \frac{1}{2^5 (2\pi)^4} \int_0^\infty k dk \frac{1}{k+\Lambda} \int_{-1}^1 dz \int_0^\pi \sin\psi_1 d\psi_1 \sin\psi_2 d\psi_2 \times (1-z^2) \exp\left[-\frac{1}{2}k(\sin\psi_1 + \sin\psi_2 - iz \cos\psi_1 - iz \cos\psi_2)\right]. \quad (\text{B3})$$

We introduce a Mellin representation by the identity

$$\frac{1}{k+\Lambda} = \frac{1}{\Lambda} \int_{\uparrow} \frac{d\eta}{2\pi i} \left( \frac{k}{\Lambda} \right)^\eta \Gamma(1+\eta) \Gamma(-\eta). \quad (\text{B4})$$

The contour  $\uparrow$  splits the poles of the  $\Gamma$  functions in Eq. (B4) and is shown in Fig. 20. Interchanging the orders of integration in Eq. (B3), and using Eq. (B4), we find

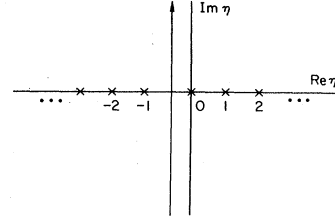


FIG. 20. The contour  $\uparrow$ .

$$\vec{J}(\vec{k}) = -\frac{1}{4\pi} \left( \hat{R} - \vec{k} \frac{1}{k^2} \vec{k} \cdot \hat{R} \right) \times \int_0^1 d\alpha e^{i(\alpha-1/2)\vec{k}\cdot\vec{R}} e^{-kR[\alpha(1-\alpha)]^{1/2}}. \quad (\text{A3})$$

Finally, if we change variables

$$\alpha = \cos^2(\frac{1}{2}\theta), \quad (\text{A4})$$

then Eq. (A3) becomes

$$\vec{J}(\vec{k}) = -\frac{1}{8\pi} \left( \hat{R} - \vec{k} \frac{1}{k^2} \vec{k} \cdot \hat{R} \right) \times \int_0^\pi \sin\theta d\theta \exp\left[\frac{1}{2}kR(i\hat{k} \cdot \hat{R} \cos\theta - \sin\theta)\right]. \quad (\text{A5})$$

#### APPENDIX B

In this appendix, we shall evaluate the integrals

$$C_1(\Lambda) = \frac{1}{2^5(2\pi)^4} \int_{\dagger} \frac{d\eta}{2\pi i} \Gamma(1+\eta)\Gamma(-\eta) \int_{-1}^1 dz \int_0^\pi \sin\psi_1 d\psi_1 \sin\psi_2 d\psi_2 \\ \times \int_0^\infty dk \Lambda^{-1-\eta} k^{\eta+1} (1-z^2) \\ \times \exp[-\frac{1}{2}k(\sin\psi_1 + \sin\psi_2 - iz \cos\psi_1 - iz \cos\psi_2)]. \quad (\text{B5})$$

The integrations over  $k$  are easily carried out with the result

$$C_1(\Lambda) = \frac{\Lambda}{2^5(2\pi)^4} \int_{\dagger} \frac{d\eta}{2\pi i} \Gamma(1+\eta)\Gamma(2+\eta)\Gamma(-\eta) \left(\frac{2}{\Lambda}\right)^{2+\eta} \\ \times \int_{-1}^1 dz \int_0^\pi \sin\psi_1 d\psi_1 \sin\psi_2 d\psi_2 (1-z^2)(\sin\psi_1 + \sin\psi_2 - iz \cos\psi_1 - iz \cos\psi_2)^{-2-\eta}. \quad (\text{B6})$$

The integral over  $z$  is

$$\int_{-1}^1 dz (1-z^2)(\sin\psi_1 + \sin\psi_2 - iz \cos\psi_1 - iz \cos\psi_2)^{-2-\eta} \\ = 2(\cos\psi_1 + \cos\psi_2)^{-2-\eta} \text{Im} \left\{ \frac{2}{\eta} \left( \frac{\sin\psi_1 + \sin\psi_2}{\cos\psi_1 + \cos\psi_2} \right) \left( \frac{\sin\psi_1 + \sin\psi_2}{\cos\psi_1 + \cos\psi_2} + i \right)^{-\eta} - \frac{1}{\eta-1} \left( \frac{\sin\psi_1 + \sin\psi_2}{\cos\psi_1 + \cos\psi_2} + i \right)^{1-\eta} \right. \\ \left. - \frac{1}{\eta+1} \left( \frac{\sin\psi_1 + \sin\psi_2}{\cos\psi_1 + \cos\psi_2} + i \right)^{-1-\eta} \left[ 1 + \left( \frac{\sin\psi_1 + \sin\psi_2}{\cos\psi_1 + \cos\psi_2} \right)^2 \right] \right\}. \quad (\text{B7})$$

In this equation,  $\text{Im}$  represents the imaginary part taken with  $\eta$  treated as if it were a real parameter.

Now, we change variables:

$$\psi_+ = \psi_1 + \psi_2, \quad (\text{B8})$$

$$\psi_- = \frac{1}{2}(\psi_1 - \psi_2). \quad (\text{B9})$$

With these new variables,

$$C_1(\Lambda) = \frac{1}{2^3(2\pi)^4} \int_{\dagger} \frac{d\eta}{2\pi i} \Gamma(1+\eta)\Gamma(2+\eta)\Gamma(-\eta)\Lambda^{-\eta-1} \\ \times \int_0^\pi d\psi_+ \int_{-\psi_+/2}^{\psi_+/2} d\psi_- [\cos^2\psi_- - \cos^2(\psi_+/2)] \cos^{-3}(\psi_+/2) \cos^{-2-\eta}\psi_- \\ \times \left\{ \frac{2}{\eta} \sin \frac{\psi_+}{2} \sin [\eta(\psi_+/2 - \pi/2)] - \frac{1}{\eta-1} \sin \left[ (\eta-1) \left( \frac{\psi_+}{2} - \frac{\pi}{2} \right) \right] \right. \\ \left. - \frac{1}{\eta+1} \sin [(\eta+1)(\psi_+/2 - \pi/2)] \right\}, \quad (\text{B10})$$

or with  $\psi_+/2 - \psi_+$ ,

$$C_1(\Lambda) = \frac{1}{2(2\pi)^4} \int_{\dagger} \frac{d\eta}{2\pi i} \Gamma(1+\eta)\Gamma(2+\eta)\Gamma(-\eta)\Lambda^{-\eta-1} \\ \times \int_0^{\pi/2} d\psi_+ \int_0^{\psi_+} d\psi_- (\cos^2\psi_- - \cos^2\psi_+) \cos^{-3}\psi_+ \cos^{-2-\eta}\psi_- \\ \times \left( \frac{2}{\eta} \sin [\eta(\psi_+ - \pi/2)] - \frac{1}{\eta-1} \sin [(\eta-1)(\psi_+ - \pi/2)] - \frac{1}{\eta+1} \sin [(\eta+1)(\psi_+ - \pi/2)] \right). \quad (\text{B11})$$

Elementary differentiation yields the identity

$$\int dx \cos^{-\alpha}x = \frac{1}{\alpha-1} \cos^{1-\alpha}x {}_2F_1\left(\frac{1}{2}, \frac{1}{2} - \frac{1}{2}\alpha; \frac{3}{2} - \frac{1}{2}\alpha; \cos^2x\right). \quad (\text{B12})$$

With the identity

$${}_2F_1\left(\frac{1}{2}, \frac{1}{2} - \frac{1}{2}\alpha; \frac{3}{2} - \frac{1}{2}\alpha; 1\right) = \frac{\Gamma(\frac{3}{2} - \frac{1}{2}\alpha)\Gamma(\frac{1}{2})}{\Gamma(1 - \frac{1}{2}\alpha)} \quad (\text{B13})$$

and Eq. (B12), the  $\psi$ -integration in Eq. (B11) can be performed to yield

$$\begin{aligned} C_1(\Lambda) = & \frac{1}{2(2\pi)^4} \int_{\dagger} \frac{d\eta}{2\pi i} \Gamma(1+\eta)\Gamma(2+\eta)\Gamma(-\eta)\Lambda^{-\eta-1} \\ & \times \int_0^{\pi/2} d\theta \left\{ \left[ \sin^{-2\eta}\theta \left( \frac{1}{\eta+1} {}_2F_1\left(\frac{1}{2}, -\frac{1}{2} - \frac{1}{2}\eta; \frac{3}{2} - \frac{1}{2}\eta; \sin^2\theta\right) - \frac{1}{\eta-1} {}_2F_1\left(\frac{1}{2}, \frac{1}{2} - \frac{1}{2}\eta; \frac{3}{2} - \frac{1}{2}\eta; \sin^2\theta\right) \right) \right. \right. \\ & \left. \left. - \frac{1}{\sin\theta} \frac{1}{\eta+1} \frac{\Gamma(\frac{1}{2} - \frac{1}{2}\eta)\Gamma(\frac{1}{2})}{\Gamma(\frac{3}{2}\eta)} + \frac{1}{\sin^3\theta} \frac{1}{\eta-1} \frac{\Gamma(\frac{3}{2} - \frac{1}{2}\eta)\Gamma(\frac{1}{2})}{\Gamma(1 - \frac{1}{2}\eta)} \right] \right. \\ & \left. \times \left( \frac{2}{\eta} \cos\theta \sin\eta\theta - \frac{1}{\eta-1} \sin(\eta-1)\theta - \frac{1}{\eta+1} \sin(\eta+1)\theta \right) \right\}, \quad (\text{B14}) \end{aligned}$$

where we have let  $\theta = \pi/2 - \psi$ .

Now, we use the identities (Gradshteyn and Ryzhik 9.137.17)<sup>41</sup>

$$(\eta+1) {}_2F_1\left(\frac{1}{2}, \frac{1}{2} - \frac{1}{2}\eta; \frac{3}{2} - \frac{1}{2}\eta; \sin^2\theta\right) - (\eta-1) {}_2F_1\left(\frac{1}{2}, -\frac{1}{2} - \frac{1}{2}\eta; \frac{3}{2} - \frac{1}{2}\eta; \sin^2\theta\right) = 2 {}_2F_1\left(\frac{1}{2}, -\frac{1}{2} - \frac{1}{2}\eta; \frac{3}{2} - \frac{1}{2}\eta; \sin^2\theta\right), \quad (\text{B15})$$

and

$$2 \cos\theta \sin\eta\theta = \sin(\eta+1)\theta + \sin(\eta-1)\theta, \quad (\text{B16})$$

to rewrite Eq. (B14) as

$$\begin{aligned} C_1(\Lambda) = & \frac{1}{(2\pi)^4} \int_{\dagger} \frac{d\eta}{2\pi i} \Gamma(1+\eta)\Gamma(2+\eta)\Gamma(-\eta)\Lambda^{-\eta-1} \frac{1}{\eta} \\ & \times \int_0^{\pi/2} d\theta \left[ \left( \frac{1}{1-\eta^2} \sin^{-2\eta}\theta {}_2F_1\left(\frac{1}{2}, -\frac{1}{2} - \frac{1}{2}\eta; \frac{3}{2} - \frac{1}{2}\eta; \sin^2\theta\right) - \frac{1}{2} \frac{1}{\sin\theta} \frac{1}{\eta+1} \frac{\Gamma(\frac{1}{2} - \frac{1}{2}\eta)\Gamma(\frac{1}{2})}{\Gamma(-\frac{1}{2}\eta)} \right) \right. \\ & \left. + \frac{1}{2} \frac{1}{\sin^3\theta} \frac{1}{\eta-1} \frac{\Gamma(\frac{3}{2} - \frac{1}{2}\eta)\Gamma(\frac{1}{2})}{\Gamma(1 - \frac{1}{2}\eta)} \right] \left( \frac{\sin(\eta+1)\theta}{\eta+1} - \frac{\sin(\eta-1)\theta}{\eta-1} \right). \quad (\text{B17}) \end{aligned}$$

Using Bateman (2, 8, 12),<sup>42</sup>

$$\frac{\sin\rho\theta}{\rho} = \sin\theta \cos\theta {}_2F_1\left(1 + \frac{\rho}{2}, 1 - \frac{\rho}{2}; \frac{3}{2}; \sin^2\theta\right), \quad (\text{B18})$$

and the Mellin representation for the hypergeometric function

$${}_2F_1(\alpha, \beta; \gamma; z) = \frac{\Gamma(\gamma)}{\Gamma(\alpha)\Gamma(\beta)} \int_{\dagger} \frac{d\rho}{2\pi i} (-z)^\rho \frac{\Gamma(\rho+\alpha)\Gamma(\rho+\beta)\Gamma(-\rho)}{\Gamma(\rho+\gamma)}, \quad (\text{B19})$$

we see that

$$\frac{\sin(\eta+1)\theta}{\eta+1} - \frac{\sin(\eta-1)\theta}{\eta-1} = \eta \frac{\Gamma(\frac{3}{2})}{\Gamma(\frac{3}{2} + \frac{1}{2}\eta)\Gamma(\frac{3}{2} - \frac{1}{2}\eta)} \sin\theta \cos\theta \int_{\dagger} \frac{d\rho}{2\pi i} \sin^{2\rho}\theta e^{i\rho\pi} \frac{\Gamma(\frac{1}{2} + \rho + \frac{1}{2}\eta)\Gamma(\frac{1}{2} + \rho - \frac{1}{2}\eta)}{\Gamma(\rho + \frac{3}{2})} \Gamma(1 - \rho). \quad (\text{B20})$$

In the above equation we shall take  $\dagger$  to be a contour parallel to the imaginary  $\rho$  axis with  $1 > \text{Re}(\rho) > \frac{1}{2}$ .

With the identity of Eq. (B20), Eq. (B17) for  $C_1(\Lambda)$  is

$$C_1(\Lambda) = \frac{1}{(2\pi)^4} \int_{\dagger} \frac{d\eta}{2\pi i} \int_{\dagger} \frac{d\rho}{2\pi i} \Lambda^{-\eta-1} e^{i\pi\rho} \frac{\Gamma(1+\eta)\Gamma(2+\eta)\Gamma(-\eta)\Gamma(\frac{3}{2})\Gamma(\frac{1}{2}+\rho+\frac{1}{2}\eta)\Gamma(\frac{1}{2}+\rho-\frac{1}{2}\eta)\Gamma(1-\rho)}{\Gamma(\frac{3}{2}+\frac{1}{2}\eta)\Gamma(\frac{3}{2}-\frac{1}{2}\eta)\Gamma(\rho+\frac{3}{2})} \\ \times \int_0^{\pi/2} d\theta \sin^{2\rho+1}\theta \cos\theta \left( \frac{\sin^{-2-\eta}\theta}{1-\eta^2} {}_2F_1\left(\frac{1}{2}, -\frac{1}{2}-\frac{1}{2}\eta; \frac{3}{2}-\frac{1}{2}\eta; \sin^2\theta\right) \right. \\ \left. - \frac{1}{2\sin\theta} \frac{\Gamma(\frac{1}{2}-\frac{1}{2}\eta)\Gamma(\frac{1}{2})}{(\eta+1)\Gamma(-\frac{1}{2}\eta)} + \frac{1}{2\sin^3\theta} \frac{\Gamma(\frac{3}{2}-\frac{1}{2}\eta)\Gamma(\frac{1}{2})}{(\eta-1)\Gamma(1-\frac{1}{2}\eta)} \right). \quad (\text{B21})$$

Under the substitution

$$z = \sin^2\theta, \quad (\text{B22})$$

this equation becomes

$$C_1(\Lambda) = \frac{1}{2(2\pi)^4} \int_{\dagger} \frac{d\eta}{2\pi i} \int_{\dagger} \frac{d\rho}{2\pi i} (\Lambda)^{-\eta-1} e^{i\pi\rho} \frac{\Gamma(1+\eta)\Gamma(2+\eta)\Gamma(-\eta)\Gamma(\frac{3}{2})\Gamma(\frac{1}{2}+\rho+\frac{1}{2}\eta)\Gamma(\frac{1}{2}+\rho-\frac{1}{2}\eta)\Gamma(1-\rho)}{\Gamma(\frac{3}{2}+\frac{1}{2}\eta)\Gamma(\frac{3}{2}-\frac{1}{2}\eta)\Gamma(\rho+\frac{3}{2})} \\ \times \int_0^1 dz z^\rho \left( \frac{z^{-1-\eta/2}}{1-\eta^2} {}_2F_1\left(\frac{1}{2}, -\frac{1}{2}-\frac{1}{2}\eta; \frac{3}{2}-\frac{1}{2}\eta; z\right) \right. \\ \left. - \frac{1}{2} z^{-1/2} \frac{\Gamma(\frac{1}{2}-\frac{1}{2}\eta)\Gamma(\frac{1}{2})}{(\eta+1)\Gamma(-\frac{1}{2}\eta)} + \frac{1}{2} z^{-3/2} \frac{\Gamma(\frac{3}{2}-\frac{1}{2}\eta)\Gamma(\frac{1}{2})}{(\eta-1)\Gamma(1-\frac{1}{2}\eta)} \right). \quad (\text{B23})$$

Using Bateman (2.4.5),<sup>42</sup>

$$\int_0^1 dz z^{a/2-\omega-1} {}_2F_1(a, b; c; z) = \frac{\Gamma(c)\Gamma(1-b)\Gamma(\frac{1}{2}a+\omega)\Gamma(\frac{1}{2}a-\omega)}{\Gamma(a)\Gamma(c-\frac{1}{2}a+\omega)\Gamma(1-b+\frac{1}{2}a-\omega)} \\ - \frac{\Gamma(c)\Gamma(1-b)}{\Gamma(1+a-b)\Gamma(c-a)} \int_0^1 dz z^{a/2+\omega-1} {}_2F_1(a, 1-c+a; 1-b+a; z), \quad (\text{B24})$$

and the identity

$${}_2F_1\left(-\frac{1}{2}-\frac{1}{2}\eta, -1; -\frac{1}{2}\eta; z\right) = 1 - \left(1 + \frac{1}{\eta}\right) z, \quad (\text{B25})$$

the integrations over  $z$  may be performed with the result

$$C_1(\Lambda) = -\frac{1}{2^5(2\pi)^3} \int_{\dagger} \frac{d\eta}{2\pi i} \int_{\dagger} \frac{d\rho}{2\pi i} (\Lambda)^{-\eta-1} e^{i\pi\rho} \frac{\Gamma(1+\eta)\Gamma(2+\eta)\Gamma(-\eta)\Gamma(\frac{1}{2}+\rho+\frac{1}{2}\eta)\Gamma(\rho-\frac{1}{2}\eta)\Gamma(1-\rho)}{(\rho^2-\frac{1}{4})\Gamma(\frac{3}{2}+\frac{1}{2}\eta)\Gamma(\frac{3}{2}-\frac{1}{2}\eta)\Gamma(\rho+\frac{3}{2})}. \quad (\text{B26})$$

With this integral representation, we see that  $C_1(\Lambda)$  possesses the Taylor-series expansion

$$C_1(\Lambda) = \frac{1}{(4\pi)^3} \left( \sum_{p=0}^{\infty} \frac{\Lambda^p \alpha_p}{p!} + \ln\Lambda \sum_{p=0}^{\infty} \frac{\Lambda^p \beta_p}{p!} \right). \quad (\text{B27})$$

(We shall calculate the coefficients  $\alpha_p$  and  $\beta_p$  in Appendix C.)

For large  $\Lambda$ ,  $C_1(\Lambda)$  has the asymptotic expansion

$$C_1(\Lambda) = \frac{1}{(4\pi)^3} \left( \sum_{p=1}^N \frac{1}{\Lambda^p} \gamma_p + \ln\Lambda \sum_{p=1}^N \frac{1}{\Lambda^p} \delta_p \right). \quad (\text{B28})$$

(We shall calculate the first few terms in this asymptotic series in Appendix D.)

#### APPENDIX C

In this appendix we shall calculate the coefficients  $\alpha_p$  and  $\beta_p$  in the series expansion for  $C_1(\Lambda)$  [cf. Eq. (B27)]. To do this, we use double Mellin integral representation of Eq. (B26),

$$C_1(\Lambda) = -\frac{1}{2^5(2\pi)^3} \int_{\dagger} \frac{d\eta}{2\pi i} \int_{\dagger} \frac{d\rho}{2\pi i} (\Lambda)^{-\eta-1} e^{i\pi\rho} \frac{\Gamma(1+\eta)\Gamma(2+\eta)\Gamma(-\eta)\Gamma(\frac{1}{2}+\rho+\frac{1}{2}\eta)\Gamma(\rho-\frac{1}{2}\eta)\Gamma(1-\rho)}{(\rho^2-\frac{1}{4})\Gamma(\frac{3}{2}+\frac{1}{2}\eta)\Gamma(\frac{3}{2}-\frac{1}{2}\eta)\Gamma(\rho+\frac{3}{2})}. \quad (\text{C1})$$

To begin we deform the  $\rho$  contour to the right in the complex  $\rho$  plane and find

$$C_1(\Lambda) = \frac{1}{2^5(2\pi)^3} \int_{\dagger} \frac{d\eta}{2\pi i} (\Lambda)^{-\eta-1} \frac{\Gamma(1+\eta)\Gamma(2+\eta)\Gamma(1-\eta)}{\Gamma(\frac{3}{2}+\frac{1}{2}\eta)\Gamma(\frac{3}{2}-\frac{1}{2}\eta)} \sum_{k=0}^{\infty} \frac{\Gamma(\frac{3}{2}+\frac{1}{2}\eta+k)\Gamma(1-\frac{1}{2}\eta+k)}{(k+\frac{3}{2})(k+\frac{1}{2})\Gamma(k+\frac{5}{2})\Gamma(k+1)}. \tag{C2}$$

The  $\eta$  contour is deformed to the left in the complex  $\eta$  plane, with the result

$$C_1(\Lambda) = \frac{1}{2^5(2\pi)^3} \sum_{p=0}^{\infty} \sum_{k=0}^{\infty} \frac{\Lambda^p}{\Gamma(p+1)} \frac{\Gamma(1+k-\frac{1}{2}p)\Gamma(\frac{3}{2}+k+\frac{1}{2}p)}{(k+\frac{3}{2})(k+\frac{1}{2})\Gamma(k+\frac{5}{2})\Gamma(k+1)\Gamma(1-\frac{1}{2}p)\Gamma(2+\frac{1}{2}p)} \times (1+p\{\ln\Lambda - \psi(p+1) + \frac{1}{2}[\psi(1-\frac{1}{2}p) - \psi(2+\frac{1}{2}p)] - \frac{1}{2}[\psi(1+k-\frac{1}{2}p) - \psi(\frac{3}{2}+k+\frac{1}{2}p)]\}). \tag{C3}$$

We now turn to finding explicit results for the coefficients in

$$C_1(\Lambda) = \frac{1}{(4\pi)^3} \left( \sum_{p=0}^{\infty} \frac{\Lambda^p \alpha_p}{p!} + \ln\Lambda \sum_{p=1}^{\infty} \frac{\Lambda^p \beta_p}{p!} \right). \tag{C4}$$

We first consider the coefficients  $\beta_p$ . For odd  $p$ , these coefficients are

$$\beta_{2n+1} = \frac{(-1)^n}{\pi(2n+3)} \sum_{k=0}^{\infty} \frac{(k+n+1)\cdots(k+1)}{(k+\frac{3}{2})(k+\frac{1}{2})[(k+\frac{3}{2})\cdots(k+\frac{1}{2}-n)]}. \tag{C5}$$

The summand may be decomposed into partial fractions and the sum over  $k$  converted into Euler dilogarithms. After some straightforward algebra, we find

$$\beta_{2n+1} = \frac{1}{\pi(2n+3)} \left\{ \frac{\Gamma(n+\frac{3}{2})}{\Gamma(\frac{1}{2})\Gamma(n+1)} \left[ \frac{\pi^2}{2} \left( 1 - \frac{1}{2(n+1)(n+\frac{1}{2})} \right) + \frac{2}{(n+1)(n+\frac{1}{2})} + 2 \left( \frac{1}{n+\frac{1}{2}} + \cdots + \frac{1}{\frac{3}{2}} + \frac{1}{n} + \cdots + \frac{1}{1} \right) \right] + \sum_{j=1}^{n-1} (-1)^j \left[ \frac{(n+j+\frac{3}{2})\cdots(j+\frac{3}{2})}{j!(n-1-j)!(j+1)^2(j+2)^2} \left( \frac{1}{j+\frac{1}{2}} + \cdots + \frac{1}{\frac{3}{2}} \right) \right] \right\}. \tag{C6}$$

For even  $p$ , we have

$$\beta_{2n+2} = \frac{2}{3} \frac{\Gamma(n+\frac{5}{2})}{(n+2)\Gamma(\frac{5}{2})\Gamma(n+1)} {}_3F_2 \left( -n, \frac{5}{2}+n, \frac{1}{2}; \frac{5}{2}, \frac{5}{2}; 1 \right). \tag{C7}$$

A list of the coefficients  $\beta_p$  is given in Table I.

Finally, there are the coefficients  $\alpha_p$ . The odd coefficients are

$$\alpha_{2n+1} = \alpha_{2n+1}^{(1)} + \alpha_{2n+1}^{(2)}, \tag{C8}$$

where

$$\alpha_{2n+1}^{(1)} = -\beta_{2n+1} \left( \frac{1}{2n+3} + \psi(2n+2) \right), \tag{C9}$$

and

$$\alpha_{2n+1}^{(2)} = \frac{(-1)^n}{2\pi(2n+3)} \sum_{k=0}^{\infty} \frac{(k+n+1)\cdots(k+1)}{(k+\frac{3}{2})(k+\frac{1}{2})[(k+\frac{3}{2})\cdots(k+\frac{1}{2}-n)]} [\psi(k+n+2) - \psi(k+\frac{1}{2}-n)]. \tag{C10}$$

TABLE I. The coefficients  $\alpha_p$  and  $\beta_p$  for  $p = 0, \dots, 10$ .

$p$	$\alpha_p$	$\beta_p$
0	0.266 299	
1	0.073 091	0.212 207
2	-0.224 261	0.333 333
3	-0.457 439	0.387 335
4	-0.602 447	0.400 000
5	-0.682 167	0.393 399
6	-0.726 537	0.380 952
7	-0.754 449	0.367 990
8	-0.785 430	0.355 555
9	-0.792 668	0.343 666
10	-0.796 744	0.332 468

We have not succeeded in finding a finite sum representation for  $\alpha_{2n+1}^{(2)}$ , as we did in the case of the coefficients  $\beta_p$ . For even  $p$ , we have

$$\alpha_{2n+2} = \alpha_{2n+2}^{(1)} + \alpha_{2n+2}^{(2)}, \tag{C11}$$

where

$$\alpha_{2n+2}^{(1)} = -\beta_{2n+2} \left( \frac{1}{2n+4} + \frac{1}{2} \psi(n+1) - \frac{1}{2n+3} - \frac{1}{2n+1} - \frac{1}{2} \psi(n+\frac{1}{2}) + \psi(2n+3) \right), \tag{C12}$$

and where

$$\alpha_{2n+2}^{(2)} = \frac{1}{4(n+2)} \frac{\Gamma(n+\frac{5}{2})}{\Gamma(n+1)\Gamma(\frac{5}{2})} \sum_{k=1}^{\infty} \frac{[(k-n-1)\cdots(-n)][(k+\frac{3}{2}+n)\cdots(n+\frac{5}{2})]}{(k+\frac{3}{2})(k+\frac{1}{2})[(k+\frac{3}{2})\cdots\frac{5}{2}][k\cdots 1]} \times \left( \frac{1}{k+n+\frac{3}{2}} + \cdots + \frac{1}{n+\frac{3}{2}} - \frac{1}{k-n-1} - \cdots - \frac{1}{-n} \right). \tag{C13}$$

Considerable use of partial fractions gives this sum as the finite sum

$$\alpha_{2n+2}^{(2)} = \frac{1}{4(n+2)} \left\{ \sum_{k=1}^n \left[ \frac{(-)^k (k+\frac{3}{2}+n)\cdots(k+\frac{5}{2})}{k!(k+\frac{3}{2})(k+\frac{1}{2})(n-k)!} \left( \frac{1}{k+\frac{3}{2}+n} + \cdots + \frac{1}{\frac{5}{2}+n} + \frac{1}{n} + \cdots + \frac{1}{1} \right) \right. \right. \\ \left. \left. + \frac{4}{3} \frac{\Gamma(n+\frac{5}{2})[\psi(n+1) - \psi(1)]}{\Gamma(\frac{5}{2})\Gamma(n+1)} + \frac{\Gamma(n+1)\Gamma(\frac{5}{2})}{\Gamma(n+\frac{5}{2})} \left( \frac{1}{n+\frac{3}{2}} + \cdots + \frac{1}{\frac{1}{2}} - 2 \ln 2 \right) \right. \right. \\ \left. \left. - \frac{\Gamma(n+2)\Gamma(\frac{3}{2})}{\Gamma(n+\frac{3}{2})} \left( \frac{1}{n+\frac{1}{2}} + \cdots + \frac{1}{\frac{1}{2}} - 2 \ln 2 \right) \right\}. \tag{C14}$$

The coefficients  $\alpha_p$  are given in Table I. The coefficients  $\alpha_p$  and  $\beta_p$  are plotted vs  $p$  in Figs. 21 and 22.

APPENDIX D

In this appendix, we shall calculate the coefficients of the asymptotic expansion of  $C_1(\Lambda)$ . To derive this asymptotic expansion, we rewrite Eq. (C2) as (C2) as

$$C_1(\Lambda) = \frac{1}{2^3(2\pi)^4} \int_{\Gamma} \frac{d\eta}{2\pi i} (\Lambda)^{-\eta-1} \left( \frac{\pi}{\sin \frac{1}{2} \pi \eta} \right)^2 \frac{\Gamma(\eta+1)}{\eta-1} \sum_{k=0}^{\infty} (-)^k \frac{\Gamma(\frac{3}{2} + \frac{1}{2} \eta + k)}{(k+\frac{3}{2})(k+\frac{1}{2})\Gamma(\frac{1}{2} \eta - k)\Gamma(k+\frac{5}{2})\Gamma(k+1)}. \tag{D1}$$

To evaluate  $C_1$  for asymptotically large  $\Lambda$ , we close the  $\eta$  contour to the right in the complex  $\eta$  plane. This procedure yields an expansion in powers of  $\Lambda^{-1}$  and  $\ln \Lambda$  multiplied by powers of  $\Lambda^{-1}$ . The first term in this series is proportional to  $1/\Lambda$ . The terms up to and including order  $1/\Lambda^3$  are

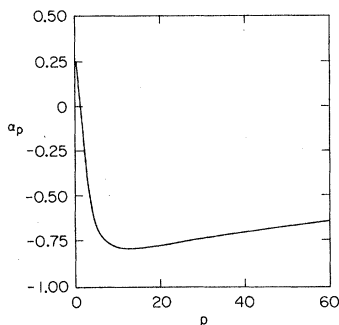


FIG. 21. The coefficients  $\alpha_p$ .

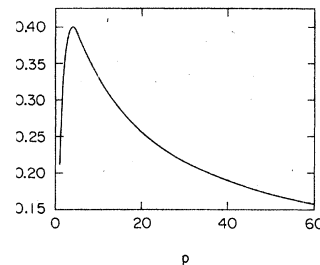


FIG. 22. The coefficients  $\beta_p$ .

$$C_1(\Lambda) = \frac{1}{(4\pi)^3} \left[ \frac{6}{\pi} \left( 1 - \frac{\pi^2}{12} \right) \frac{1}{\Lambda} - \frac{1}{\Lambda^2} + \frac{16}{3\pi} \frac{1}{\Lambda^3} (\ln\Lambda + \gamma - 1) \right] + O(\ln\Lambda/\Lambda^4). \quad (D2)$$

In this equation  $\gamma$  is Euler's constant.

#### APPENDIX E

In this appendix we obtain an integral representation for

$$\vec{\mathcal{A}}(\vec{r}) \equiv \int \frac{d^3k}{(2\pi)^3 2k} \vec{\psi}(\vec{k}) e^{i\vec{k}\cdot\vec{r}}, \quad (E1)$$

and for the transverse electric and magnetic fields. With these integral representations, we may find the energy and charge densities generated by the gluon cloud corresponding to  $\vec{\psi}$ .

Using Eqs. (3.19), (4.2), and (4.3) of I, and (A5) of this paper, we have

$$\vec{\mathcal{A}}(\vec{r}) = -\frac{1}{8\pi C_2^{1/2}(\Lambda)} \int \frac{d^3k}{(2\pi)^3 2k} (\vec{i} - \hat{k}\hat{k}) \cdot \hat{R} \frac{1}{k+\Lambda} e^{i\vec{k}\cdot\vec{r}} \int_0^\pi \sin\psi d\psi e^{(kR/2)(i\hat{k}\cdot\hat{R}\cos\psi - \sin\psi)}, \quad (E2)$$

with

$$\vec{m} \equiv \vec{r} + \frac{1}{2} \vec{R} \cos\psi \quad (E3)$$

and

$$x \equiv k |\vec{m}|. \quad (E4)$$

A little algebra shows that

$$\vec{\mathcal{A}}(\vec{r}) = -\frac{1}{4(2\pi)^3 C_2^{1/2}(\Lambda)} \int_0^\infty dk \int_0^\pi \sin\psi d\psi \frac{k}{k+\Lambda} e^{-kR/2 \sin\psi} \{ [j_0(x) - j_1(x)/x] \hat{R} + \hat{m}\hat{m} \cdot \hat{R} [3j_1(x)/x - j_0(x)] \}. \quad (E5)$$

In this equation the spherical Bessel function of the  $l$ th is  $j_l(x)$ . Letting

$$\vec{\mathcal{A}}(\vec{r}) = \hat{r} \mathcal{G}_r + \hat{R} \mathcal{G}_R, \quad (E6)$$

we have

$$\mathcal{G}_r = -\frac{1}{4(2\pi)^3 C_2^{1/2}(\Lambda)} \int_0^\infty dk \int_0^\pi \sin\psi d\psi \frac{k}{k+\Lambda} e^{-kR/2 \sin\psi} \frac{r(\frac{1}{2}R \cos\psi + r \cos\theta)}{(\frac{1}{4}R^2 \cos^2\psi + Rr \cos\psi \cos\theta + r^2)} \left( \frac{3j_1(x)}{x} - j_0(x) \right), \quad (E7)$$

and

$$\mathcal{G}_R = -\frac{1}{4(2\pi)^3 C_2^{1/2}(\Lambda)} \int_0^\infty dk \int_0^\pi \sin\psi d\psi \frac{k}{k+\Lambda} e^{-kR/2 \sin\psi} \times \left( [j_0(x) - j_1(x)/x] + \frac{\frac{1}{2}R \cos\psi (\frac{1}{2}R \cos\psi + r \cos\theta)}{(\frac{1}{4}R^2 \cos^2\psi + Rr \cos\psi \cos\theta + r^2)} [3j_1(x)/x - j_0(x)] \right). \quad (E8)$$

The equations for  $\vec{\mathcal{E}}_1$  are identical to Eqs. (D6)–(D8) except that

$$\frac{k}{k+\Lambda} \rightarrow \frac{k^2}{k+\Lambda}. \quad (E9)$$

We also find that

$$\vec{\mathcal{E}} = \frac{1}{4(2\pi)^3 C_2^{1/2}(\Lambda)} (\hat{r} \times \hat{R}) \int_0^\infty dk \int_0^\pi \sin\psi d\psi \frac{k^2}{k+\Lambda} \frac{\vec{r}}{|\vec{r} + \frac{1}{2} \vec{R} \cos\psi|} e^{-kR/2 \sin\psi} j_1(x). \quad (E10)$$

- <sup>1</sup>T. Appelquist, M. Dine, and I. Muzinich, Phys. Lett. 69B, 231 (1977); Phys. Rev. D 17, 2074 (1978).
- <sup>2</sup>F. Feinberg, Phys. Rev. Lett. 39, 316 (1977); Phys. Rev. D 17, 2659 (1978).
- <sup>3</sup>W. Fischler, Nucl. Phys. B129, 157 (1977).
- <sup>4</sup>E. Poggio, Phys. Rev. D 16, 2586 (1977).
- <sup>5</sup>S. Davis and F. Feinberg, Phys. Lett. 78B, 90 (1978).
- <sup>6</sup>S. L. Adler, Phys. Rev. D 17, 3212 (1978); 18, 411 (1978); 19, 1168 (1979); 19, 2997 (1979); 20, 1386 (1979).
- <sup>7</sup>R. C. Giles and L. McLerran, Phys. Lett. 79B, 447 (1978).
- <sup>8</sup>R. C. Giles and L. McLerran, Phys. Rev. D 19, 3732 (1979).
- <sup>9</sup>N. H. Parsons and P. Senjanovic, Phys. Lett. 79B, 273 (1978).
- <sup>10</sup>P. Cvitanović, R. J. Gonsalves, and D. E. Neville, Phys. Rev. D 18, 3881 (1978).
- <sup>11</sup>G. Domokos and S. Kovesi-Domokos, Phys. Rev. D 19, 2984 (1979).
- <sup>12</sup>J. J. Aubert *et al.*, Phys. Rev. Lett. 33, 1404 (1974).
- <sup>13</sup>J. E. Augustin *et al.*, Phys. Rev. Lett. 33, 1406 (1974).
- <sup>14</sup>G. S. Abrams *et al.*, Phys. Rev. Lett. 33, 1453 (1974).
- <sup>15</sup>W. Braunschweig *et al.*, Phys. Lett. 57B, 407 (1975).
- <sup>16</sup>G. J. Feldman *et al.*, Phys. Rev. Lett. 35, 821 (1975).
- <sup>17</sup>W. M. Tannenbaum *et al.*, Phys. Rev. Lett. 35, 1323 (1975).
- <sup>18</sup>S. W. Herb *et al.*, Phys. Rev. Lett. 39, 252 (1977).
- <sup>19</sup>W. R. Innes *et al.*, Phys. Rev. Lett. 39, 1240 (1977).
- <sup>20</sup>C. W. Darden *et al.*, Phys. Lett. 78B, 364 (1978).
- <sup>21</sup>B. J. Harrington, S. Y. Park, and A. Yildiz, Phys. Rev. Lett. 34, 168 (1975); 34, 706 (1975).
- <sup>22</sup>E. Eichten *et al.*, Phys. Rev. Lett. 34, 369 (1975).
- <sup>23</sup>J. S. Kang and H. J. Schnitzer, Phys. Rev. D 12, 841 (1975); 12, 2791 (1975).
- <sup>24</sup>J. Rosner, H. Thacker, and C. Quigg, Phys. Rev. D 18, 274 (1978); 18, 287 (1978).
- <sup>25</sup>J. H. Richardson, Phys. Lett. 82B, 272 (1979).
- <sup>26</sup>I. B. Khriplovich, Zh. Eksp. Teor. Fiz. 74, 37 (1978) [Sov. Phys.—JETP 47, 18 (1978)].
- <sup>27</sup>S. Tomonaga, Prog. Theor. Phys. 2, 6 (1947).
- <sup>28</sup>T. D. Lee and D. Pines, Phys. Rev. 92, 883 (1953).
- <sup>29</sup>T. D. Lee and R. Christian, Phys. Rev. 74, 1760 (1959).
- <sup>30</sup>M. H. Friedman, T. D. Lee, and R. Christian, Phys. Rev. 100, 1494 (1955).
- <sup>31</sup>E. M. Henley and T. D. Lee, Phys. Rev. 101, 1536 (1956).
- <sup>32</sup>M. Dine, Phys. Lett. 81B, 339 (1979).
- <sup>33</sup>L. S. Brown and W. I. Weisberger, Phys. Rev. D 20, 3239 (1979).
- <sup>34</sup>E. Eichten and F. Feinberg, Phys. Rev. Lett. 43, 1205 (1979).
- <sup>35</sup>V. N. Gribov, Nucl. Phys. B139, 1 (1978).
- <sup>36</sup>S. Mandelstam, Washington APS Meeting, 1977 (unpublished).
- <sup>37</sup>J. E. Mandula, Phys. Lett. 67B, 175 (1977).
- <sup>38</sup>P. Sikivie and N. Weiss, Phys. Rev. Lett. 40, 1411 (1978).
- <sup>39</sup>C. G. Callan, R. Dashen, D. J. Gross, F. Wilczek, and A. Zee, Phys. Rev. D 18, 4684 (1978).
- <sup>40</sup>G. P. Lepage, J. Comput. Phys. 27, 192 (1978).
- <sup>41</sup>I. S. Gradshteyn and I. M. Ryzhik, *Tables of Integrals, Series, and Products* (Academic, New York, 1965).
- <sup>42</sup>*Higher Transcendental Functions* (Bateman Manuscript Project), edited by A. Erdelyi (McGraw-Hill, New York, 1953).